



This is a repository copy of *PLL-less three-phase droop-controlled inverter with inherent current-limiting property*.

White Rose Research Online URL for this paper:
<http://eprints.whiterose.ac.uk/155482/>

Version: Accepted Version

Proceedings Paper:

Dedeoglu, S. and Konstantopoulos, G.C. orcid.org/0000-0003-3339-6921 (2019) PLL-less three-phase droop-controlled inverter with inherent current-limiting property. In: IECON 2019 - 45th Annual Conference of the IEEE Industrial Electronics Society. IECON 2019 - 45th Annual Conference of the IEEE Industrial Electronics Society, 14-17 Oct 2019, Lisbon, Portugal. IEEE , pp. 4013-4018. ISBN 9781728148793

<https://doi.org/10.1109/iecon.2019.8927219>

© 2019 IEEE. Personal use of this material is permitted. Permission from IEEE must be obtained for all other users, including reprinting/ republishing this material for advertising or promotional purposes, creating new collective works for resale or redistribution to servers or lists, or reuse of any copyrighted components of this work in other works. Reproduced in accordance with the publisher's self-archiving policy.

Reuse

Items deposited in White Rose Research Online are protected by copyright, with all rights reserved unless indicated otherwise. They may be downloaded and/or printed for private study, or other acts as permitted by national copyright laws. The publisher or other rights holders may allow further reproduction and re-use of the full text version. This is indicated by the licence information on the White Rose Research Online record for the item.

Takedown

If you consider content in White Rose Research Online to be in breach of UK law, please notify us by emailing eprints@whiterose.ac.uk including the URL of the record and the reason for the withdrawal request.



eprints@whiterose.ac.uk
<https://eprints.whiterose.ac.uk/>

PLL-Less Three-Phase Droop-Controlled Inverter with Inherent Current-Limiting Property

Seyfullah Dedeoglu and George C. Konstantopoulos

Dept. of Automatic Control and Systems Engineering

The University of Sheffield

Sheffield, S1 3JD, UK

{sdedeoglu1, g.konstantopoulos}@sheffield.ac.uk

Abstract—In this paper, a novel droop control method for three-phase grid-connected inverters is proposed to guarantee closed-loop system stability and an inherent current-limiting property without the need of a PLL. The inverter is connected to the grid via a filter and a line. Based on the synchronously rotating dq frame modelling and nonlinear ultimate boundedness theory, it is analytically proven that the proposed control scheme maintains the inverter current below a certain upper bound. This current limitation is guaranteed independently of the grid, line and filter parameters; thus increasing the controller robustness. In addition, asymptotic stability of the desired equilibrium point of the closed-loop system is guaranteed under different values of the proposed controller gain. To verify the effectiveness of the proposed nonlinear control strategy, extensive simulations are realized using Matlab/Simulink, where both the stability and the current-limiting property of the controller are validated.

Index Terms—Nonlinear control, current limitation, reference frame, stability analysis, three-phase inverter, PLL-less implementation

I. INTRODUCTION

Due to the increase in the power demand with the technological advancements, the use of the renewable energy sources in the power production becomes more and more important to decrease the undesirable effects to the environment caused by conventional power generation [1]–[4]. Renewable energy sources can be both integrated into the traditional grid and connected to distributed microgrids where they can operate either in grid connected or in islanded mode [5], [6]. For the integration of these renewable energy sources, three-phase inverters are being used and represent essential devices to control the active and reactive power, support the grid by operating similar to conventional synchronous generators through droop control, and maintain the system states (e.g. current, voltage and frequency) within a given range to ensure system stability [7]–[9].

In grid-connected applications, the droop control methodology is used to control the power inverters and provide grid voltage and frequency support by adjusting the real and reactive power injected by the renewable sources [10]–[12]. The control of real and reactive power injected to the grid can be accomplished separately by introducing additional terms in the droop control structure to remove their coupling [13], while virtual impedance methods can be added as well to affect the inverter output or line impedance in order to enhance

the stability of the grid [14]. Depending on the type of the output impedance, the droop expressions can take the form of $P-\omega/Q-V$ (inductive impedance) and $P-V/Q-\omega$ (resistive impedance) and they are used to support the local voltage and frequency of the system at the point of common coupling (PCC) [15], while a line is generally considered between the PCC and the main grid.

Grid synchronization is one of the most critical issues that needs to be considered in grid-connected applications to maintain a stable and reliable operation of a grid-tied inverter [16]. In this process, many methods such as Kalman Filter, nonlinear least square, and phase locked loops (PLL) can be used. Due to its easy implementation and simplicity, the most commonly used method is the PLL. Although PLLs can be very effective in balanced grid conditions, it has been shown in the literature that they can lead to undesirable phenomena and instability of the system in distorted grid conditions [17]. In order to overcome these problems, self-synchronization algorithms have been recently proposed and can be embedded in the droop control [18], [19].

To increase the reliability of the grid-connected inverter operation and meet the requirements dictated by the grid authority [5], [20], the relationship between the inverter and grid should be managed by considering the protection and stability issues [21], [22]. For instance, when injecting power to the grid, the system states such as voltage, current and frequency should be limited for stability and power balance purposes. Particularly, current limitation is of major importance under grid faults or sudden changes of the supply, demand or the desired reference signal received from a supervisory control. To achieve current limitation, PI controllers with limiters and saturation blocks are often used [23]–[26]. However, these techniques can cause the well-known integrator windup problem, and eventually system instability. Even when anti-windup methods are used to overcome this issue, they require information of the system parameters to ensure rigorous closed-loop system stability, which may not be available or may vary in a real applications [27], [28]. To this end, the bounded integral controller [29] using nonlinear input-to-state stability theory has been proposed to deal with the integrator windup problems and it has been successfully implemented to limit the system current

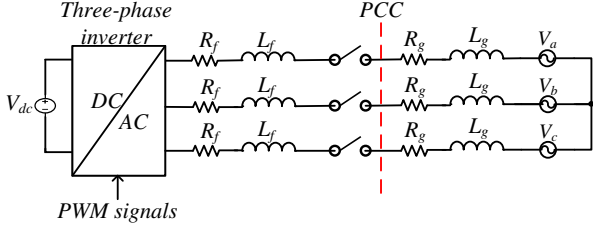


Fig. 1. Three-phase grid-connected inverter.

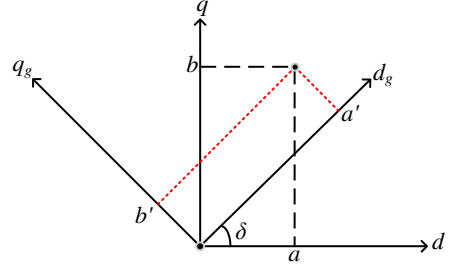


Fig. 2. Axis transformation.

in both three-phase [30] and single-phase applications [31]. Nevertheless, asymptotic stability of the closed-loop system to a desired equilibrium point has not been proven yet for a three-phase inverter connected to the PCC, while a PLL is often required for the implementation that reduces system reliability.

In this paper, a novel nonlinear current-limiting droop controller for a three-phase inverter connected to the grid through a filter and a distribution line is proposed without the need of a PLL. The proposed controller supports the voltage and frequency of the PCC and inherently limits the current of the inverter using only local measurements of the PCC independently from unrealistic values of the reference power. The desired current limitation is mathematically proven using nonlinear ultimate boundedness theory and closed-loop asymptotic stability is examined using small-signal model analysis. The system is modelled using the synchronous rotating (dq) frame, and for the stability analysis, a global-to-local axis transformation is used to investigate asymptotic convergence to a desired equilibrium point [32]. To verify the theoretical analysis and the effectiveness of the novel control design, detailed simulation results are presented for a three-phase grid-connected inverter.

The rest of the paper is arranged as follows. In Section II, the system dynamics are given and the main problem is defined. In Section III, the design process of the nonlinear current-limiting controller is explained in detail. In Section IV, the current-limiting property and the closed-loop system stability are examined. In Section V, simulation results are provided, and in Section VI, the conclusions of the paper are presented.

II. PROBLEM DEFINITION AND SYSTEM DYNAMICS

The system under consideration is a three-phase inverter connected to a point of common coupling (PCC) through a filter, as demonstrated in Fig. 1. The filter resistance and inductance are described as R_f and L_f , respectively, whereas the line between the PCC and the main grid has a resistance R_g and inductance L_g . The inverter dc input voltage is expressed as V_{dc} , and the three-phase grid voltages are given as

$$\begin{bmatrix} V_a \\ V_b \\ V_c \end{bmatrix} = \begin{bmatrix} V_m \cos(\omega_g t) \\ V_m \cos(\omega_g t - 120^\circ) \\ V_m \cos(\omega_g t + 120^\circ) \end{bmatrix},$$

with V_m and ω_g being the grid voltage amplitude and frequency, respectively.

In order to realize the system analysis, an algebraic axis

transformation [32] is used to align the grid and inverter voltages as shown in Fig. 2. The algebraic transformation is given below [32]:

$$\begin{bmatrix} a \\ b \end{bmatrix} = \begin{bmatrix} \cos(\delta) & -\sin(\delta) \\ \sin(\delta) & \cos(\delta) \end{bmatrix} \begin{bmatrix} a' \\ b' \end{bmatrix}. \quad (1)$$

In this context, (1) is referred as global-to-local transformation, where δ represents the rotation angle. If the rotation is counterclockwise then $\delta > 0$, and if it is clockwise, as in the proposed system, then $\delta < 0$. For the clockwise case, the rotation matrix (1) (after δ is replaced with $-\delta$) becomes

$$\begin{bmatrix} \cos(\delta) & \sin(\delta) \\ -\sin(\delta) & \cos(\delta) \end{bmatrix}, \quad (2)$$

where $\delta = \theta - \theta_g$, which represents the difference between the inverter and grid angles. Assuming that the PCC voltage is aligned on the d_g axis of the global dq reference frame and neglecting the small voltage drop and phase shifting caused by the line, i.e. $V_{gd}' = V_m$ and $V_{gq}' = 0$, then by using the inverse of the rotation matrix (1), the inverter side equivalence of the PCC voltages can be found as

$$\begin{bmatrix} V_{gd} \\ V_{gq} \end{bmatrix} = \begin{bmatrix} V_m \cos(\delta) \\ -V_m \sin(\delta) \end{bmatrix}. \quad (3)$$

As a result, the three-phase dynamics in the local dq reference frame are expressed as

$$L_f \frac{dI_d}{dt} = -R_f I_d + \omega L_f I_q - V_{gd} + V_d \quad (4)$$

$$L_f \frac{dI_q}{dt} = -R_f I_q - \omega L_f I_d - V_{gq} + V_q \quad (5)$$

where I_d, I_q and V_d, V_q represent the dq frame inverter currents and voltages. Active power (P) and reactive power (Q) can be calculated as in [32]

$$P = \frac{3}{2} (V_{gd} I_d + V_{gq} I_q), Q = \frac{3}{2} (V_{gq} I_d - V_{gd} I_q). \quad (6)$$

It is clear from (3) and (6) that the P and Q expressions include nonlinear terms, and any control method that controls the real and reactive power injected by the inverter, such as the droop control method, will result in a nonlinear closed-loop system. Therefore, nonlinear control theory should be considered to prove key system features, such as current limitation, and guarantee a reliable operation. To this end, the main aim of this paper is to design a nonlinear controller which limits the system current even when there is excessive power demand, and ensure the system stability at all times.

III. PROPOSED NONLINEAR CURRENT-LIMITING CONTROLLER

The main focus of this paper is to design a nonlinear controller which limits the inverter injected current, and realizes the desired power droop functions without the need of a PLL. For this purpose, the local inverter voltages (V_d and V_q), which represent the control inputs of the system are proposed to take the form

$$V_d = V_{gd} + E_d - r_v I_d - \omega L_f I_q \quad (7)$$

$$V_q = V_{gq} - r_v I_q + \omega L_f I_d \quad (8)$$

where E_d and r_v act as a controllable virtual voltage used as a controller state, and a constant virtual resistance used to limit the current, respectively. Motivated by the recently proposed bounded integral controller [29], the E_d dynamics of the proposed nonlinear controller are defined as

$$\dot{E}_d = c_d [(E^* - V_{rms}) - n(Q - Q_{set})] E_{dq}^2 \quad (9)$$

$$\begin{aligned} \dot{E}_{dq} = & -c_d \frac{E_d E_{dq}}{E_{max}^2} [(E^* - V_{rms}) - n(Q - Q_{set})] \\ & - \left(\frac{E_d^2}{E_{max}^2} + E_{dq}^2 - 1 \right) E_{dq} \end{aligned} \quad (10)$$

where E_{dq} is the additional controller state to create a two-dimensional plane with E_d as in [29], while c_d and E_{max} are positive constants related to the dynamics of the bounded integral controller. The initial conditions of the controller states are selected as $E_{d0} = 0$ and $E_{dq0} = 1$. The proposed control dynamics has been suitably designed to guarantee that the controller states remain bounded in the ranges $E_d \in [-E_{max}, E_{max}]$ and $E_{dq} \in [0, 1]$. For the proof of the boundedness, the reader is referred to [19], [29], [30]. Note that if the expression $(E^* - V_{rms}) - n(Q - Q_{set})$ becomes zero at the steady-state in the proposed controller then the $Q \sim V$ droop control is realized. E^* is the nominal RMS grid voltage, V_{rms} is the inverter RMS voltage calculated as $V_{rms} = \sqrt{\frac{V_{gd}^2 + V_{gq}^2}{2}} = \frac{V_m}{\sqrt{2}}$, Q_{set} is the reactive power reference value and n is the reactive power droop coefficient. Finally, the $P \sim \omega$ droop is accomplished independently from the controller dynamics (9) and (10) and employed through the expression

$$\omega = \omega^* - m(P - P_{set}) \quad (11)$$

where ω is the inverter angular frequency which is used in the dq transformation, ω^* is the nominal angular frequency, m is the active power droop coefficient, and P_{set} is the active power reference value. Note that since only the local variables are used in the power calculation and the controller dynamics, then the proposed design does not require any information after the PCC. Additionally, before connecting to the grid, there is $E_d = E_{d0} = 0$, $I_d = I_q = 0$ and hence from (7) and (8) there is $V_d = V_{gd}$ and $V_q = V_{gq}$ which can be equivalently implemented using the abc quantities without a PLL. Hence, a PLL is not needed neither before nor after the grid connection.

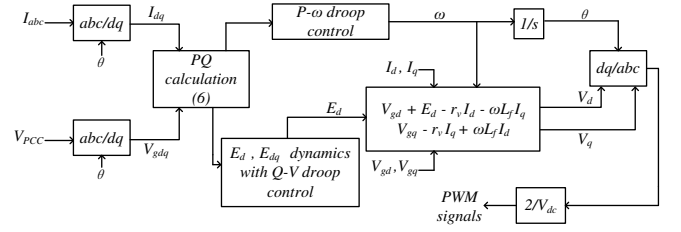


Fig. 3. Implementation of the system.

IV. CURRENT-LIMITING PROPERTY AND CLOSED-LOOP STABILITY ANALYSIS

A. Current-limiting property

The closed-loop system can be obtained by replacing the proposed controller dynamics (7) and (8) in the inverter dynamics (4) and (5) as

$$L_f \frac{dI_d}{dt} = -(R_f + r_v)I_d + E_d \quad (12)$$

$$L_f \frac{dI_q}{dt} = -(R_f + r_v)I_q \quad (13)$$

From (13), it becomes clear that if initially $I_q(0) = 0$ then $I_q(t) = 0, \forall t \geq 0$. Hence, in order to guarantee the desired current limitation, it is sufficient to prove using nonlinear control theory that only the d-axis current (I_d) will be limited at all times below a given value I_{max} . For this purpose, if the energy stored in the filter inductor is used as a candidate Lyapunov function

$$V = \frac{1}{2} L_f I_d^2, \quad (14)$$

the time derivative of (14) can be calculated using (12) as

$$\begin{aligned} \dot{V} = & -(R_f + r_v)I_d^2 + E_d I_d \\ \leq & -(R_f + r_v)I_d^2 + |E_d| |I_d|. \end{aligned} \quad (15)$$

Since $E_d \in [-E_{max}, E_{max}]$ from the boundedness of the controller states, then (15) can be written as,

$$\dot{V} \leq -(R_f + r_v)I_d^2 + E_{max} |I_d| \quad (16)$$

Thus,

$$\dot{V} \leq -R_f I_d^2, \forall |I_d| \geq \frac{E_{max}}{r_v} \quad (17)$$

According to theorem 4.18 [33], it is proven that the solution $I_d(t)$ of (12) is ultimately bounded. Principally, if initially the system current is chosen such that $|I_d(0)| \leq \frac{E_{max}}{r_v}$, then from the ultimate boundedness theory [33], it can be resulted that

$$|I_d| \leq \frac{E_{max}}{r_v}, \forall t \geq 0. \quad (18)$$

In order to limit the current I_d below a maximum value I_{max} , then the controller parameters E_{max} and r_v can be chosen to meet the expression

$$E_{max} = r_v I_{max}. \quad (19)$$

If (19) is replaced in (18), it is verified that

$$|I_d| \leq I_{max}, \forall t \geq 0, \quad (20)$$

which confirms the desired current-limiting property.

From the above ultimate boundedness proof, it is clear that the limitation of the inverter current is guaranteed independently of the system variables, such as the grid frequency and voltage, or the parameters of the filter or the line. In addition, the current-limiting property is guaranteed during the entire grid-connected inverter operation, even during transients. In contrast to the existing approaches in the literature that use additional saturation units and might suffer from integrator windup and instability [24], [25], here the proposed controller introduces an inherent anti-windup property due to the bounded integral control structure, thus facilitating the stability analysis of the closed-loop system which follows in the next section.

B. Small-signal stability analysis

Although the current-limiting property is proven analytically in the previous section using nonlinear systems theory, the asymptotic stability of the closed-loop to a desired equilibrium point has not been examined, yet. Therefore, this section emphasizes on evaluating the asymptotic performance of the proposed controller using small-signal stability analysis for a three-phase grid-connected inverter equipped with the proposed current-limiting droop controller. After adding the controller states (9) and (10) into the system and considering $\delta = \omega - \omega_g = \Delta\omega$, the state vector of the closed-loop system becomes $x = [I_d \ E_d \ \delta \ I_q \ E_{dq}]^T$. Consider an equilibrium point $x_e = [I_{de} \ E_{de} \ \delta_e \ I_{qe} \ E_{dqe}]^T$, where $E_{de} \in (-E_{max}, E_{max})$ and $E_{dqe} \in (0, 1]$. Then the Jacobian matrix of the closed-loop system can be constructed as in (21). As can be understood from (13) and the system Jacobian matrix (21) that the q axis current I_q is controlled to be 0 and results in a negative eigenvalue $-\frac{(R_f+r_v)}{L_f}$. Similarly, the term $-2E_{dqe}^2$ is always negative, since E_{dqe} is considered to be in the range $E_{dqe} \in (0, 1]$. To this end, the equilibrium point x_e of the closed-loop system will be asymptotically stable, if the eigenvalues of the matrix J_T (22) have negative real parts.

$$J = \begin{bmatrix} J_T & 0_{3 \times 1} & 0_{3 \times 1} \\ 0_{1 \times 3} & -\frac{(R_f+r_v)}{L_f} & 0 \\ C_{1 \times 3} & 0 & -2E_{dqe}^2 \end{bmatrix} \quad (21)$$

$$C^T = \begin{bmatrix} -\frac{3c_d E_{de} E_{dqe} V_m \sin(\delta_e)}{2E_{max}^2} \\ -\frac{2E_{de} E_{dqe}}{E_{max}^2} \\ -\frac{3c_d E_{de} E_{dqe} V_m \cos(\delta_e) i_{de}}{2E_{max}^2} \end{bmatrix}$$

$$J_T = \begin{bmatrix} -\frac{(R_f+r_v)}{L_f} & \frac{1}{L_f} & 0 \\ A \sin(\delta_e) & 0 & A \cos(\delta_e) i_{de} \\ -B \cos(\delta_e) & 0 & B \sin(\delta_e) i_{de} \end{bmatrix} \quad (22)$$

In the matrix J_T , the terms A and B are given as $\frac{3}{2}V_m c_d n E_{dqe}^2$ and $\frac{3}{2}m V_m$, respectively. In order to calculate

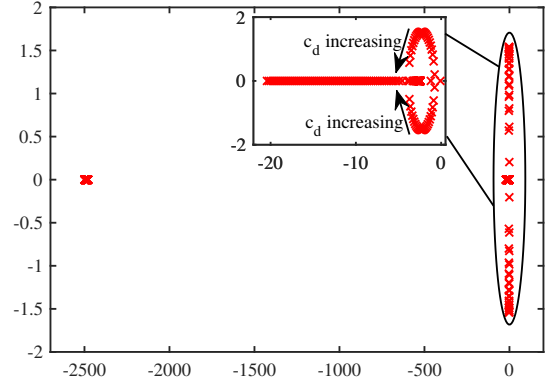


Fig. 4. Closed-loop system eigenvalues as a function of controller gain c_d with $0.1 \leq c_d \leq 50$

the equilibrium point values of I_{de} , E_{de} , δ_e and E_{dqe} , the equations (9), (10), (11), and (12) can be used. In Fig. 4, a root locus analysis is realized by changing the controller gain c_d between 0.1 and 50 using the system parameters in Table I. Contrary to [34] which assumes the equilibrium points are constant while changing the droop coefficients, the controller gain c_d changes only the convergence rate of the system states to the equilibrium points. As it can be easily observed, the closed-loop system stability is guaranteed for any value of the controller gain in the given range verifying the effectiveness of the proposed controller to both limit the inverter current and regulate the system at the desired equilibrium point.

TABLE I
SIMULATION PARAMETERS OF THE SYSTEM

Parameters	Values	Parameters	Values
L_f, L_g	2.2mH	S_{max}	3300VA
R_f, R_g	0.5Ω	r_v	5Ω
n	0.0167	m	9.52×10^{-4}
ω^*	2π50	V_{dc}	700V
E_{max}	27.5	I_{max}	5A
c_d	15	E^*	220V

V. SIMULATION RESULTS

In order to validate the performance of the proposed controller, a three-phase inverter connected to the grid through a filter and a line (Fig. 1) is simulated using the Matlab/Simulink software. The implementation diagram of the proposed controller is provided in Fig. 3 and the simulation parameters are given in Table I. The main aims in this section are:

- To verify the desired droop control operation and convergence to the desired equilibrium points under changes of the real and reactive power references,
- To illustrate that the inverter currents can never exceed the defined upper limit even under extreme power demands.

During the operation, droop control is implemented for both active and reactive power. Initially, the accurate active power regulation is achieved since $\omega_g = \omega^*$, while the $Q - V$ droop is enabled for the reactive power as explained in the controller design. At the time instant $t = 0$, P is set to 1000W and Q is set to 1000Var. However, even if P is regulated exactly

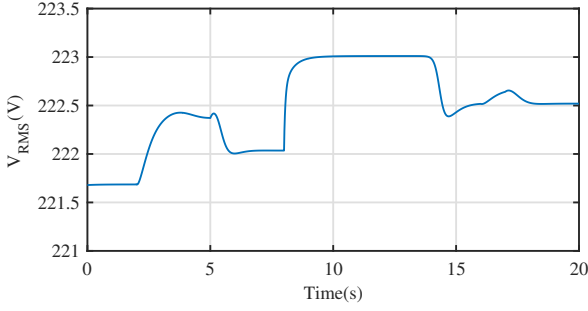


Fig. 5. RMS voltage.

at P_{set} as expected when $\omega_g = \omega^*$, Q is regulated to a lower value that can be calculated using $\frac{E^* - V_{rms}}{n} + Q_{set}$. The change in the RMS voltage of the system is given in Fig. 5 where the difference between the rated voltage E^* and V_{rms} can be clearly observed. At $t = 2s$, P_{set} is increased to 2000W and at $t = 5s$, it drops to 1500W. It is clear from the Fig. 6 that P follows the exact P_{set} values as expected. At the time instant $t = 8s$, the reactive power reference is set to an extreme value which is 2200Var to check the effectiveness of the designed controller. Since the droop mode is enabled, the expected steady-state value for Q can be calculated as 2020Var. However, it cannot go beyond 1828Var as can be seen from Fig. 6, due to the inherent current-limiting property of the proposed controller. At this point, the current I_d attempts to exceed its maximum value $I_{max} = 5A$, but the controller limits the current to protect the inverter as rigorously proven using ultimate boundedness theory and as seen in Fig. 7. At $t = 12s$, Q_{set} is decreased to 1500Var, and after some transient the reactive power is regulated to 1350Var as shown in Fig. 6. To test the $P \sim -\omega$ droop operation, the grid frequency is decreased by 0.03Hz at $t = 16s$ and restored at $t = 17s$. The active power then changes to 1700W and is restored back to 1500W after 1s as shown in Fig. 6 to compensate the change in the grid frequency.

Since P and Q are coupled due to their expressions (6), there are some fluctuations when either of them changes. However, this does not affect the current-limiting property as shown in Fig. 7, according to the rigorous mathematical proof. Thus, the capability of the proposed droop controller has been tested for different power reference values and it has been validated that, even under unrealistic power demand, both the closed-loop stability and the current-limiting property are maintained at all times.

In order to confirm the theoretical analysis, the time domain response of the controller states E_d and E_{dq} is given in Fig. 8. It can be clearly seen that the controller states remain on the defined limits during the entire operation. When the reactive power demand increases to an high value, then E_d and E_{dq} tend to E_{max} and 0, respectively, to ensure that the inverter current I_d remains lower than I_{max} .

VI. CONCLUSIONS

In this paper, a new nonlinear PLL-less current-limiting controller is proposed for a three-phase grid-connected inverter.

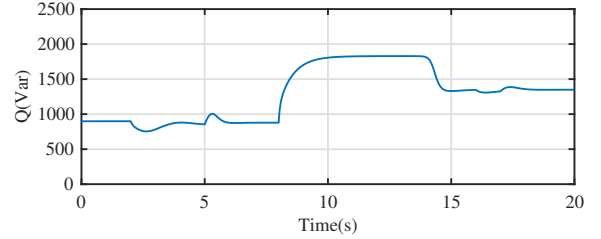
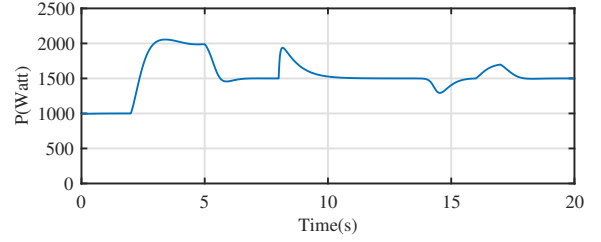


Fig. 6. Active and reactive power.

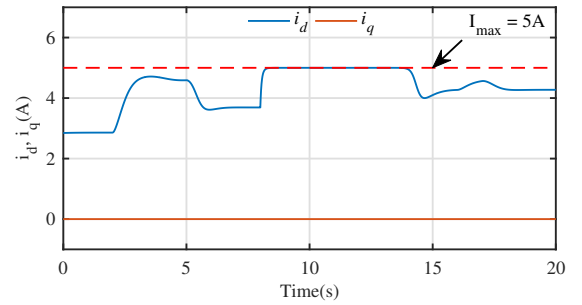


Fig. 7. d- and q-axis currents.

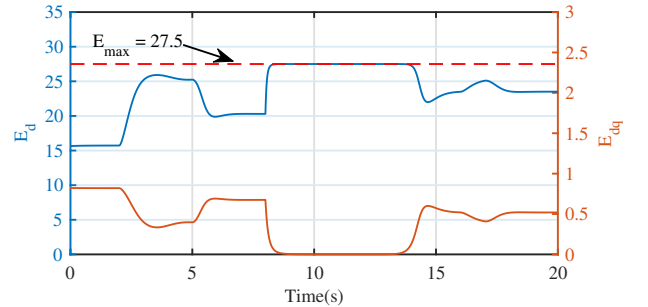


Fig. 8. Response of the controller states.

The controller is proposed using the synchronously rotating (dq) frame of the inverter. Voltage support and frequency support are realized at the PCC point by including the droop dynamics into the nonlinear controller dynamics. Considering the nonlinear dynamics of the system, the current-limiting property is proven for the injected inverter current using nonlinear ultimate boundedness theory. In addition, closed-loop system stability is guaranteed for different values of the controller gains. The proposed controller performance and its stability properties are confirmed via detailed simulation results.

ACKNOWLEDGEMENT

This work is supported by the EPSRC under Grants No. EP/S001107/1 and EP/S031863/1.

REFERENCES

- [1] M. Liserre, T. Sauter, and J. Y. Hung, "Future energy systems: Integrating renewable energy sources into the smart power grid through industrial electronics," *IEEE Ind. Electron. Mag.*, vol. 4, no. 1, pp. 18–37, 2010.
- [2] J. M. Carrasco et al., "Power Electronic Systems for the Grid Integration of Renewable Energy Sources: A Survey," *IEEE Trans. Ind. Electron.*, vol. 53, no. 4, pp. 1002–1016, 2006.
- [3] M. Mutarraf, Y. Terriche, K. Niazi, J. Vasquez, and J. Guerrero, *Energy Storage Systems for Shipboard Microgrids—A Review*, vol. 11, no. 12, 2018.
- [4] M. Dreidy, H. Mokhlis, and S. Mekhilef, "Inertia response and frequency control techniques for renewable energy sources: A review," *Renew. Sustain. Energy Rev.*, vol. 69, no. November 2015, pp. 144–155, 2017.
- [5] P. T. Manditereza and R. Bansal, "Renewable distributed generation: The hidden challenges - A review from the protection perspective," *Renew. Sustain. Energy Rev.*, vol. 58, pp. 1457–1465, 2016.
- [6] A. Ipakchi and F. Albuyeh, "Grid of the future," *IEEE Power Energy Mag.*, vol. 7, no. 2, pp. 52–62, 2009.
- [7] Q.-C. Zhong, T. Hornik, *Control of Power Inverters in Renewable Energy and Smart Grid Integration*, New York, NY, USA: Wiley-IEEE Press, 2013.
- [8] J. Liu, L. Zhou, X. Yu, B. Li, and C. Zheng, "Design and analysis of an LCL circuit-based three-phase grid-connected inverter," *IET Power Electron.*, vol. 10, no. 2, pp. 232–239, 2017.
- [9] S. A. Khajehoddin, M. Karimi-Ghartemani, and M. Ebrahimi, "Grid-supporting inverters with improved dynamics," *IEEE Trans. Ind. Electron.*, vol. 66, no. 5, pp. 3655–3667, 2019.
- [10] Y. Sun, X. Hou, J. Yang, H. Han, M. Su, and J. M. Guerrero, "New Perspectives on Droop Control in AC Microgrid," *IEEE Trans. Ind. Electron.*, vol. 64, no. 7, pp. 5741–5745, 2017.
- [11] X. Meng, J. Liu, and Z. Liu, "A generalized droop control for grid-supporting inverter based on comparison between traditional droop control and virtual synchronous generator control," *IEEE Trans. Power Electron.*, vol. PP, no. c, pp. 1–1, 2018.
- [12] J. Liu, S. Member, Y. Miura, and T. Ise, "Comparison of Dynamic Characteristics Between Virtual Synchronous Generator and Droop Control in Inverter-Based Distributed Generators," vol. 31, no. 5, pp. 3600–3611, 2016.
- [13] U. B. Tayab, M. A. Bin Roslan, L. J. Hwai, and M. Kashif, "A review of droop control techniques for microgrid," *Renew. Sustain. Energy Rev.*, vol. 76, no. November 2016, pp. 717–727, 2017.
- [14] Q. C. Zhong and Y. Zeng, "Universal Droop Control of Inverters with Different Types of Output Impedance," *IEEE Access*, vol. 4, pp. 702–712, 2016.
- [15] L. Huang, H. Xin, Z. Wang, L. Zhang, K. Wu, and J. Hu, "Transient Stability Analysis and Control Design of Droop-Controlled Voltage Source Converters Considering Current Limitation," *IEEE Trans. Smart Grid*, vol. 10, no. 1, pp. 578–591, 2019.
- [16] M. Ashabani, F. D. Freijedo, S. Golestan, and J. M. Guerrero, "Inducverters: PLL-Less Converters With Auto-Synchronization and Emulated Inertia Capability," *IEEE Trans. Smart Grid*, vol. 7, no. 3, pp. 1660–1674, 2016.
- [17] N. Jaalam, N. A. Rahim, A. H. A. Bakar, C. K. Tan, and A. M. A. Haidar, "A comprehensive review of synchronization methods for grid-connected converters of renewable energy source," *Renew. Sustain. Energy Rev.*, vol. 59, pp. 1471–1481, 2016.
- [18] Q. C. Zhong, P. L. Nguyen, Z. Ma, and W. Sheng, "Self-synchronized synchronverters: Inverters without a dedicated synchronization unit," *IEEE Trans. Power Electron.*, vol. 29, no. 2, pp. 617–630, 2014.
- [19] G. C. Konstantopoulos, Q. C. Zhong, and W. L. Ming, "PLL-Less Nonlinear Current-Limiting Controller for Single-Phase Grid-Tied Inverters: Design, Stability Analysis, and Operation under Grid Faults," *IEEE Trans. Ind. Electron.*, vol. 63, no. 9, pp. 5582–5591, 2016.
- [20] E. M. G. Rodrigues, G. J. Osório, R. Godina, A. W. Bizuayehu, J. M. Lujano-Rojas, and J. P. S. Catalão, "Grid code reinforcements for deeper renewable generation in insular energy systems," *Renew. Sustain. Energy Rev.*, vol. 53, pp. 163–177, 2016.
- [21] F. Blaabjerg, R. Teodorescu, M. Liserre, and A. V. Timbus, "Overview of control and grid synchronization for distributed power generation systems," *IEEE Trans. Ind. Electron.*, vol. 53, no. 5, pp. 1398–1409, 2006.
- [22] H. J. Laaksonen, "Protection principles for future microgrids," *IEEE Trans. Power Electron.*, vol. 25, no. 12, pp. 2910–2918, 2010.
- [23] H. Xin, L. Huang, L. Zhang, Z. Wang, and J. Hu, "Synchronous Instability Mechanism of P-f Droop-Controlled Voltage Source Converter Caused by Current Saturation," *IEEE Trans. Power Syst.*, vol. 31, no. 6, pp. 5206–5207, 2016.
- [24] L. Huang et al., "A Virtual Synchronous Control for Voltage-Source Converters Utilizing Dynamics of DC-Link Capacitor to Realize Self-Synchronization," *IEEE J. Emerg. Sel. Top. Power Electron.*, vol. 5, no. 4, pp. 1565–1577, 2017.
- [25] N. Bottrell and T. C. Green, "Comparison of current-limiting strategies during fault ride-through of inverters to prevent latch-up and wind-up," *IEEE Trans. Power Electron.*, vol. 29, no. 7, pp. 3786–3797, 2014.
- [26] A. D. Paquette and D. M. Divan, "Virtual Impedance Current Limiting for Inverters in Microgrids With Synchronous Generators," *IEEE Trans. Ind. Appl.*, vol. 51, no. 2, pp. 1630–1638, 2015.
- [27] L. Zaccarian, A. R. Teel, "Nonlinear scheduled anti-windup design for linear systems," *IEEE Trans. Autom. Control*, vol. 49, no. 11, pp. 2055–2061, Nov. 2004.
- [28] S. Tarbouriech, M. Turner, "Anti-windup design: An overview of some recent advances and open problems," *IET Control Theory Appl.*, vol. 3, no. 1, pp. 1–19, Jan. 2009.
- [29] G. C. Konstantopoulos, Q. C. Zhong, B. Ren, and M. Krstic, "Bounded Integral Control of Input-to-State Practically Stable Nonlinear Systems to Guarantee Closed-Loop Stability," *IEEE Trans. Automat. Contr.*, vol. 61, no. 12, pp. 4196–4202, 2016.
- [30] Q.-C. Zhong and G. C. Konstantopoulos, "Current-Limiting Three-Phase Rectifiers," *IEEE Trans. Ind. Electron.*, vol. 65, no. 2, pp. 957–967, 2018.
- [31] Q.-C. Zhong and G. C. Konstantopoulos, "Current-Limiting Droop Control of Grid-connected Inverters," *IEEE Trans. Ind. Electron.*, vol. 0046, no. c, pp. 1–1, 2016.
- [32] M. Rasheduzzaman, J. A. Mueller, and J. W. Kimball, "An accurate small-signal model of inverter-dominated islanded microgrids using (dq) reference frame," *IEEE J. Emerg. Sel. Top. Power Electron.*, vol. 2, no. 4, pp. 1070–1080, 2014.
- [33] H. K. Khalil, *Nonlinear systems*. Upper Saddle River, NJ: Prentice Hall, 2002.
- [34] N. Pogaku, M. Prodanović, and T. C. Green, "Modeling, analysis and testing of autonomous operation of an inverter-based microgrid," *IEEE Trans. Power Electron.*, vol. 22, no. 2, pp. 613–625, 2007.